

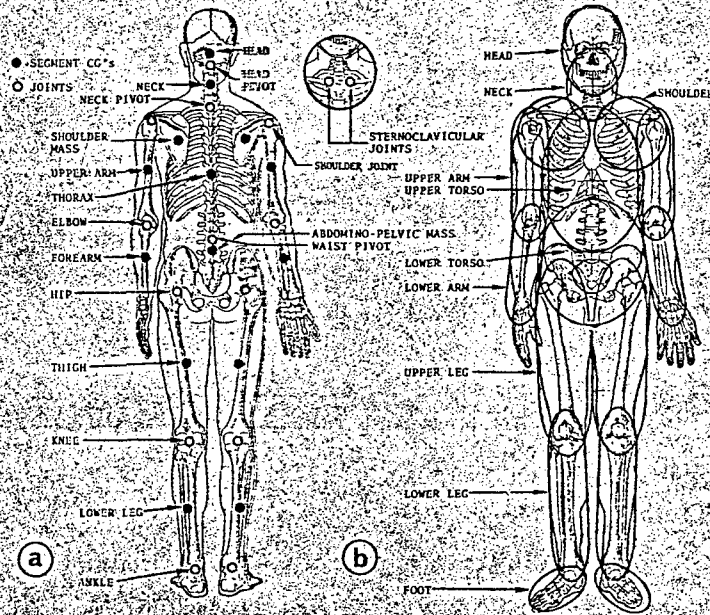
ADA 040351

The Effectiveness of Mathematical Models as a Human Analog

d

3808AN

Mathematical Modeling Biodynamic Response to Impact



SP-412



1976 SAE National Automobile
Engineering and Manufacturing Meeting
Dearborn, Michigan
October 18-22, 1976

20030113094

The Effectiveness of Mathematical Models as a Human Analog

Georg D. Frisch, Joseph O'Rourke, and Louis D'Aulerio
Crew Systems Dept.
Naval Air Development Center

3808AN

MATHEMATICAL MODELING of the dynamic response of an occupant to severe decelerative forces has become widespread in the engineering community. This is due to the dangers inherent in human testing at these levels as well as the inability to fabricate a reliable dummy that exhibits motional fidelity when compared to corresponding human responses. Satisfactory results which would establish models as a reasonable human analog have not yet been achieved. This limited success to date is due to the difficulties inherent in modeling the complexity of the various body interactions as well as the paucity of precise human data. Unacceptable simulation results of the head and neck response can usually be traced to inadequate sophistication in modeling the head and neck or to errors propagated by deficiencies in modeling the thorax - restraint system interactions.

Tracking only head motion during live human tests is insufficient for simulation validation, since one may adequately match head angular displacement in the inertial reference frame while being inaccurate in relative head-neck-torso displacements. Consequently, more than just the head segment should be monitored so that relative positions of the various instrumented segments can be established and the adequacy of the simulation ascertained on more than single segment comparison. If one assumes that the forces propagated to the head are transmitted via the first thoracic vertebral body (T1), then the forces at T1 and not the sled profile define the driving function of the head. Only when T1 is instrumented can relative motion between the head and torso be determined with precision and the simulated thoracic-restraint belt interaction verified.

This paper analyzes data on the dynamic response of the living human head and neck to -Gx (eye-balls out) impact acceleration where the motion of the subject's head and T1 was monitored in the midsagittal plane with inertial instrumentation and high speed photography for confirmation.

The Calspan "3D Computer Simulator of Motor Vehicle Crash Victims," Ultrasystems' "Crash Victim Simulator - Light Aircraft" and Boeing Computer Services' "Prometheus" were used to provide estimates of occupant responses. These three programs represent a sample of the various complexities and approaches employed in modeling biodynamic responses. Inputs to the programs were made as uniform as program restrictions allowed and outputs were compared for consistency as well as accuracy in replicating the human results obtained.

METHODS

INPUT PARAMETERS - The specific human runs selected for possible simulation were all above 10 G and relatively high G onsets (greater than 500 G/second). It was felt that at these levels the motion of the head and neck would not be influenced by muscular activity resulting from anticipation on the part of the test subjects. The subject finally chosen for simulation exhibited typical response characteristics in the head angular and head linear accelerations attained with the time histories of the various acceleration profiles being very similar to those of the group as a whole. Based on this analysis the subject was felt to be a representative sample of the response to be expected at this level of deceleration.

Detailed descriptions of the instrumenta-

ABSTRACT

This paper analyzes data on the dynamic response of the living human head and neck to -Gx impact acceleration. The Calspan "3D Computer Simulator of a Motor Vehicle Crash Victim," Ultrasystems "Crash Victim Simulator - Light Aircraft" and Boeing Computer Services "Prometheus" were used to provide estimates of the responses monitored. Inputs to the programs were made as comparable as program

restrictions would allow. Outputs were compared to each other as well as to the corresponding human test run. Program outputs proved to be consistent but failed to adequately replicate human results. Inclusion of head to neck articulation did not by itself improve results. Relocation of the head pivot away from the occipital condyles or introduction of muscular activity was indicated.

tion and methods employed have been previously presented-(1,2)*. Briefly, both external (whole body) and x-ray (head and neck) anthropometric data were obtained for the subject tested. The use of x-ray anthropometry enabled the fixing of the transducer mounts and associated instrumentation to well-defined anatomical coordinate systems (i.e., head and T1). Locations of the head C.G. and occipital condyles were established relative to the head anatomical coordinate system, permitting transformation of the transducer data to these points using rigid body mechanics. Since both the head and spine were instrumented, the corresponding head and T1 coordinate systems could be tracked in time, enabling the head angular displacement to be defined relative to both the inertial and T1 coordinate systems.

The definition of the head anatomical coordinate system and the head C.G. location were based on Walker's analysis, while the location of the occipital condyles was determined from lateral anthropometric x-rays of the test subject-(3). Similarly, the mass and mass moment of inertia of the head and neck were estimated from Walker's data and scaled to the anthropometric characteristics of the subject. The neck was defined to be a vector extending from the T1 coordinate system origin to the occipital condyle point. Since both the T1 origin and the occipital condyle point could be located in the inertial reference system throughout the run, neck angle was defined as the angle the neck made with the Z axis of this system. Head-neck (H-N) angle was taken to be the angle the neck vector made with the head anatomical coordinate system. Using this approach, precise initial conditions could be determined from photographic and x-ray data and the validity of the simulation ascertained.

The mass and mass moment of inertia, link lengths and C.G. locations of the other relevant body segments were based on Dempster's work - (4). Establishing joint locations in the various segments proved to be the most vexing problem. The occipital condyles were chosen as the articulation point between the head and neck, while the origin of the T1 coordinate system was assumed to be the pivot between the neck and thorax. Since the occipital condyles are anatomically distributed areas instead of points and are not in the midsagittal plane of the head, the precise head pivot location is somewhat inexact but was taken to be the occipital condylar point projected onto the midsagittal plane of the head. The locations of the other joints (sternoclavicular, shoulder, elbows, waist, hips, knees, ankles) were estimated by scaling Dempster's approximations. All joints were assumed to be ball and sockets with the exception of the knees and elbows, which were con-

sidered to be hinged. Limits of joint motion for the extremities and the torso were based on data from Dempster as well as Glanville and Kreezer - (5). Head range of motion was based on Glanville's, Bowman's and Tarriere's data - (6, 7). It should be noted that Glanville's forced range of motion agrees favorably with Tarrier's voluntary values whereas Bowman's results are more in keeping with Glanville's voluntary ranges (Table 1). The proportions of the total range accounted for by dorsiflexion and ventriflexion are shown in Table 2. Again, there is good agreement between Glanville and Tarriere. The total range of motion was broken down into neck-torso(N-T) and head-neck (H-N) components using Bowman's and Tarriere's analysis (Table 3). Ventriflexion values for N-T and H-N ranges are in relatively good agreement as are dorsiflexion H-N values. Dorsiflexion N-T ranges, however, show a large discrepancy, with Bowman's dorsiflexion values accounting for only 20 percent of the total N-T range of motion. The simulation values used (Table 4) were based on Tarriere's proportional breakdown of the N-T, H-N ranges applied to the averages shown in Table 1. All joints were considered to have almost free motion (i.e., only friction and viscous retarding forces) up to the joint limiting angle, where spring characteristics were introduced to restore the segment excursion back within

Table 1 - Total Range of Motion

		Glanville and Kreezer	Bowman and Robbins	Tarriere and Sapin	Average
DORSIFLEXION (Backward)	Forced	77°		100°	89.5°
	Voluntary	61°	45°		
VENTRIFLEXION (Forward)	Forced	76°		85°	60.5°
	Voluntary	60°	70°		
Total Range	Forced	153°		185°	169.0°
	Voluntary	121°	115°		

Table 2 - Proportions of Total Range of Motion

		Glanville and Kreezer	Bowman Robbins	Tarriere and Sapin	Average
DORSIFLEXION	Forced	0.5		0.54	0.52
	Voluntary	0.5	0.39		
VENTRIFLEXION	Forced	0.5		0.46	0.48
	Voluntary	0.5	0.61		

Table 3 - Neck - Torso, Neck - Head Breakdown

	N - T		N - H	
	Bowman Robbins	Tarriere and Sapin	Bowman Robbins	Tarriere and Sapin
DORSIFLEXION	15°	70°	30°	30°
VENTRIFLEXION	60°	65°	10°	20°
Range	75°	135°	40°	50°

Table 4 - Head and Neck Pivot Joint Ranges for Simulation

	N - T	N - H	Total
DORSIFLEXION	61.95°	26.55°	88.5°
VENTRIFLEXION	61.56°	18.94°	80.5°
Range	123.51°	45.49°	169.0°

* Numbers in parentheses designate References at the end of paper.

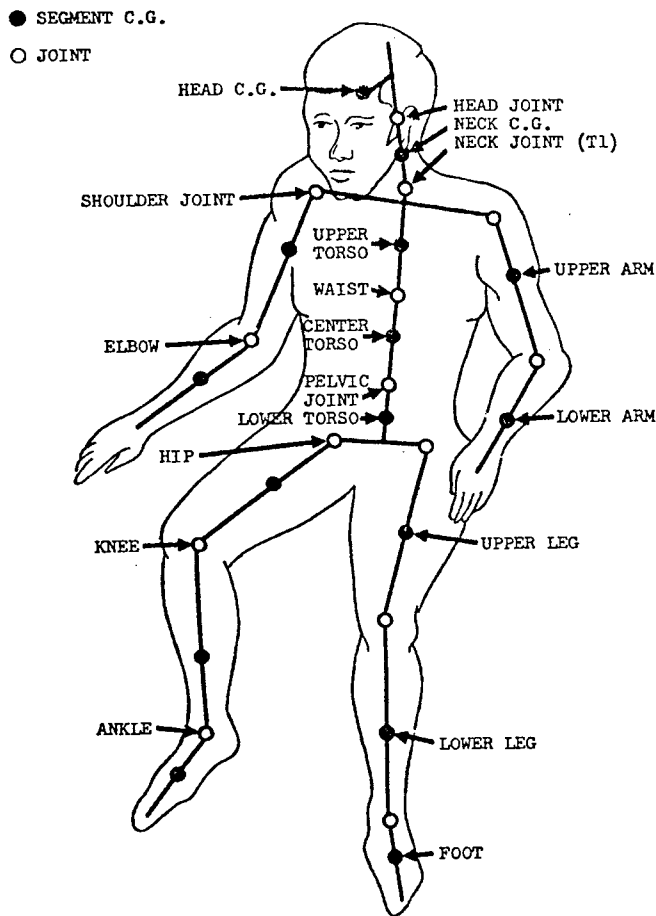


Fig. 1 - Segment c.g. and joint locations of Standard Calspan occupant model

its joint stop contour. Estimates of the N-T and H-N forcing element (spring and dashpot function) were obtained from Becker's preliminary analysis of data from the subjects tested - (8).

The dimensions of all body segment contact surfaces were based on the subject's anthropometry. Kroell's data on the impact tolerance of the human thorax was used to estimate the force deflection properties of the thorax - (9). Dynamic stress-strain curves for the restraint harness webbing were also obtained and used as inputs to the program - (10).

3D Computer Simulator of Motor Vehicle Crash Victim (CALSPAN) - This program was developed to simulate motor vehicle crash victims and extensive dummy validation efforts have been conducted - (11,12). The equations of motion are formulated in a manner that allows variation of the number of segments and joints without altering the program structure. The program is well suited to study an occupant in a high deceleration or crash environment. Interactions of the occupant with his environment (i.e., seat, restraint system, cabin configuration) are handled with sophistication and this characteristic together with its modular structure made it a prime candidate to investigate the responses observed from the test subjects.

The standard 15 segment, 14 joint version (Figure 1) was deemed inappropriate in that the entire upper torso was represented as one segment. Since a double shoulder strap restraint system was used in the runs, it would seem probable that although the shoulders were adequately restrained, the thorax and consequently T1 could exhibit greater excursion than the shoulders themselves. The configuration of the upper torso was modified with the inclusion of two sternoclavicular joints (ball and socket) and was broken down into thorax and two shoulder elements. This modification allowed the distribution of weight to be apportioned in a manner consistent with Dempster's cadaver data and required no source modification to the computer program. The various joints were located in the relevant segments (using Dempster's approximations) and this 16 segment-15 joint representation is shown in Figure 2.

It should be noted that the program has provisions for usage of a sophisticated shoulder joint model which basically consists of upper torso, scapula and upper arm segments connected via ball and socket joints and spring dampers to simulate muscles. Relative motion between the scapula and upper torso segments is limited by a fixed distance constraint, simulating the clavicle, and a rolling-sliding constraint between the respective contact surfaces. Due to the absence of reliable input data, this particular option of the program was not employed but will be considered in future simulations. Additionally, a new numerical integrator (Fleck Integrator), which appears to be substantially more efficient, has been developed by Calspan but was not used in our runs - (13). It is expected therefore that the noted execution times in this paper can be drastically reduced.

Crash Victim Simulator-Light Aircraft (Ultrasystems) - The CVSLA computer program consists of a three-dimensional model of an aircraft seat, occupant and restraint system and was developed as an aid in the design and analysis of crashworthy seats and restraint systems for general aviation aircraft. The user has the option of choosing among several basic seat designs incorporated within the program, ranging from a rigid configuration to one including provisions for simulating plastic behavior. A rigid seat was used for this simulation. The modeled restraint system consisted of a lap-belt and a double shoulder strap harness. Since this model does not consider segment deformation (as is the case for the Calspan), the force elongation properties of the shoulder strap webbing were modified to reflect the thoracic deformation that would occur when these belts are loaded. The occupant is modeled via 11 rigid segments and 10 joints (Figure 3). In the original version, joint ranges, segment dimensions and inertial properties were determined from studies of human body anthropometry and kinematics - (14). Segment properties were reduced to fixed frac-

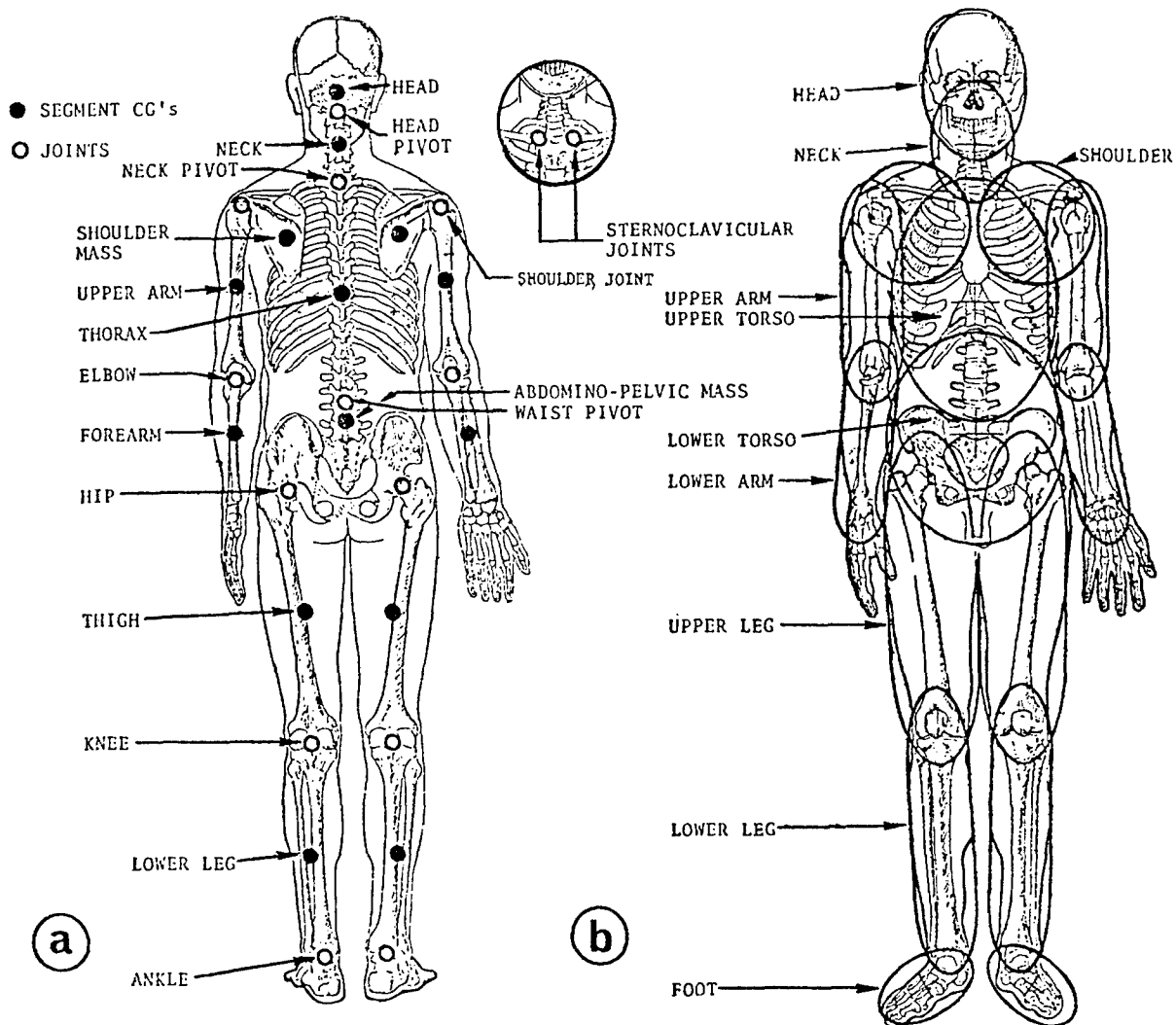


Fig. 2 - 16 segment, 15 joint representation used for modified Calspan occupant model

tions of total body weight and stature. These fractions, along with joint properties and a multiplication factor to account for total body size, are incorporated in the program and are used to calculate the occupant's anthropometric characteristics. This approach greatly reduces the inputs to the program although it precludes the modeling of a specific test subject's anthropometric characteristics.

Consequently, for purposes of this paper it became necessary to alter these fractional calculations to insure that the link lengths, mass distribution, and joint locations would approximate the subject simulated. This was accomplished without affecting the operation of the program, although it circumvented the user oriented aspects of the input. Additionally, joint ranges and loading properties were modified to agree, as close as the various methods of calculation would allow, to the inputs used in the Calspan simulation. Link length and C.G. location of the head and neck, which is modeled as a single rigid element, together with the initial condition of this segment were matched as close as possible to those of the human run. Outputs of the program

were expanded to include the accelerations of the neck link (T1) as well as the angular acceleration and velocity of the head C.G.. As a result of these modifications the only significant occupant differences from the Calspan model was the representation of the head and neck as a single segment (vs. head and neck connected by a joint) and the modeling of the upper torso as a rigid element (vs. thorax and two shoulder segments connected by two sternoclavicular joints). This results in a somewhat different distribution of masses for the upper torso and the head-neck segment, as well as decreased articulation between the thorax and the head.

Prometheus (Boeing) - This program is a two-dimensional crash victim simulator. The occupant is modeled by eight concentrated masses connected by seven links (Figure 4), and is restrained by lap and shoulder belts. The occupant interacts with the environment through a non-linear finite element model of the seat structure. The program incorporates a number of user-oriented features, and is especially useful for studying seat structure behavior during helicopter and fixed-wing

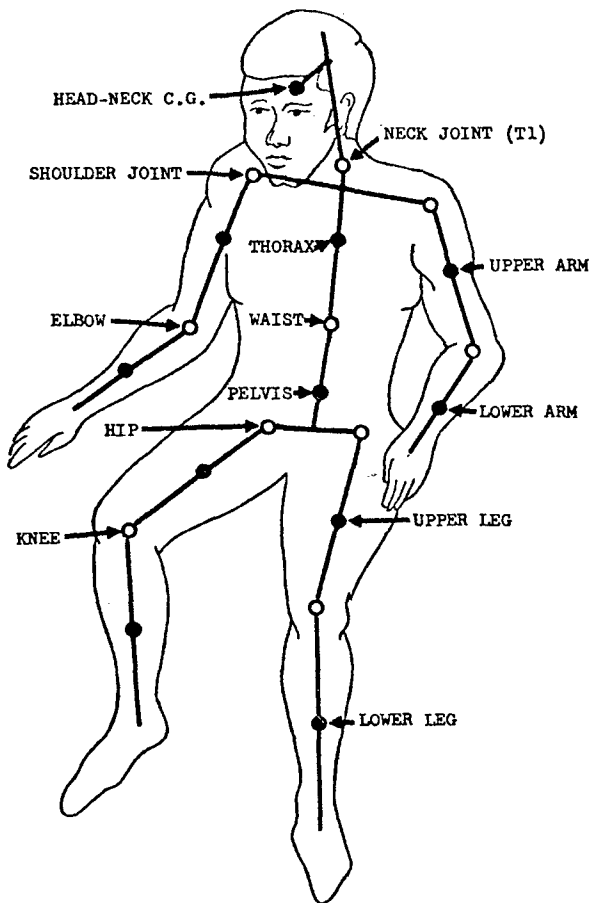


Fig. 3 - Segment c.g. and joint locations of Ultrasystems occupant model

aircraft crashes, which was its original purpose - (15). The program has recently been improved and extended beyond the version used here - (16). The flexibility of the input to Prometheus made it unnecessary to alter the program in order to match the conditions being simulated. The three-dimensional distributed mass of the occupant was apportioned to the eight two-dimensional point masses, and the single lap and shoulder belts were doubled in strength to simulate left and right straps. The head and neck parameters (neck length, head-neck mass, head-neck C.G. position) were chosen to agree with the corresponding quantities for the Calspan head and neck segment combined. The neck joint parameters and the user-defined belt force-deflection properties were selected to match the Calspan functions as closely as possible.

Accuracy of Numerical Integration -

In order to insure that possible differences in results from the three simulators were not due to lack of stability in the respective numerical integration procedures, the programs were checked for precision of results over several error levels and integration step sizes for all relevant variables. The three computer programs use similar integration schemes for numerically solving the differential equations. Calspan employs an exponential integrator whereas CVSLA uses a fourth order predictor -

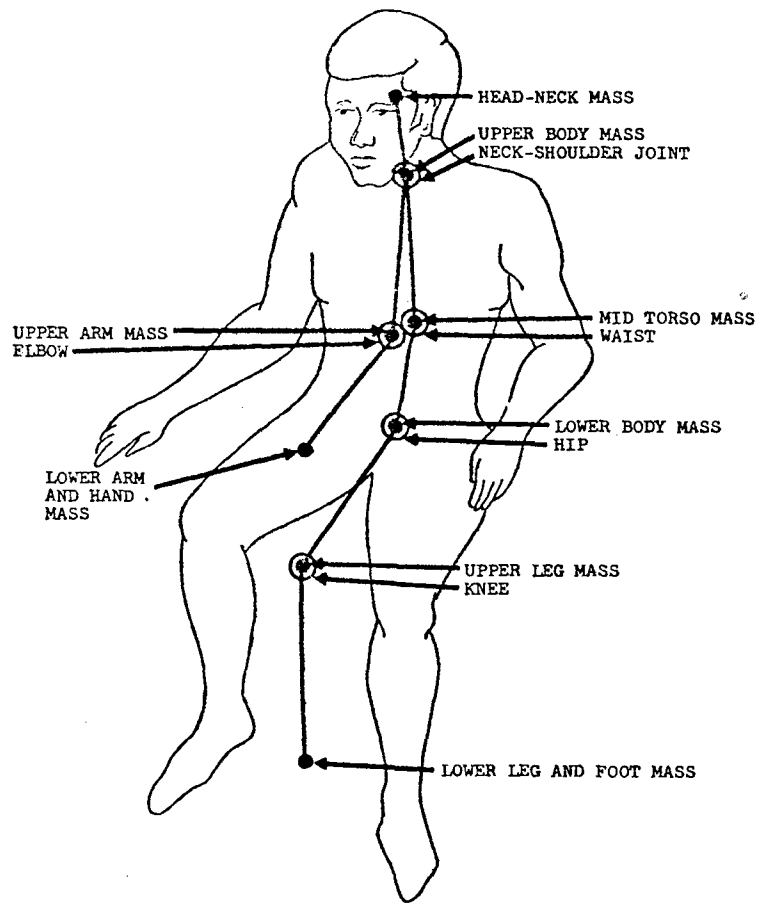


Fig. 4 - Mass distribution and joint locations of Boeing Computer Services occupant model

corrector and Prometheus a third order predictor-corrector. All three schemes employed use a variable integration step size. Integration accuracy is mainly controlled by two parameters: the minimum integration step size and the ratio test limit. During the calculation of an integration step, the relative error between the predicted and corrected derivatives is compared to the specified ratio limit. If the error is greater than the limit, the step is rejected and the integration is attempted again with a smaller step size. This process is repeated until either the ratio test is passed or the time step becomes smaller than the minimum step size. Calspan employs a three level check which also tests the absolute magnitude of the derivative vector as well as the magnitude of the error, but the parameters for these other checks were set to low values, insuring failure of these tests and forcing reliance on the ratio test. If the integration solutions are stable and convergent, then reducing the ratio test limits should not alter the results significantly.

All three programs were run with the inputs held constant but with different ratio test limits. CVSLA was run for ratio tests of 0.1, 0.05, and 0.01, using minimum step sizes of 0.1, 0.1, and 0.01 ms. respectively. Likewise, Prometheus was checked for ratio tests of 0.1, 0.05, and 0.01, using a minimum step size of 0.01 ms. throughout. Since Calspan runs routinely used

SIM H182.9.80-PK.530G/S ONSET.

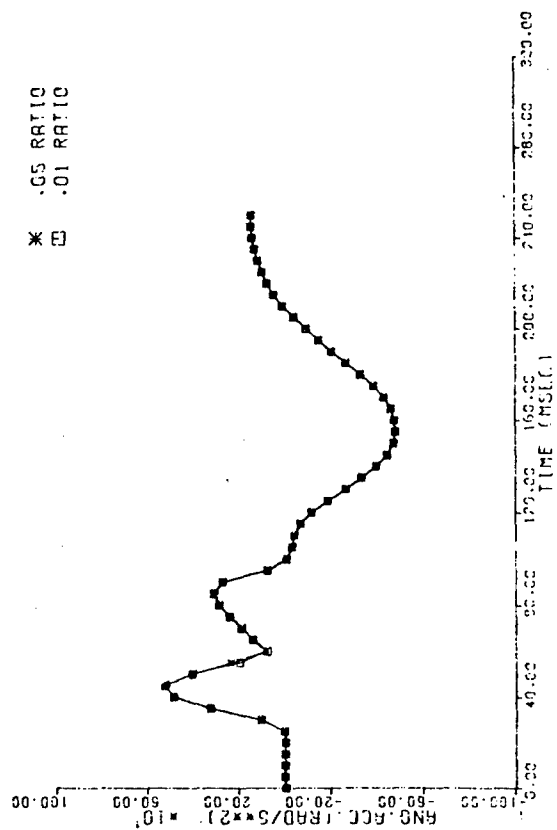


Fig. 5 - Ratio test comparison for head angular acceleration results (Calspan)

SIM H182.9.80-PK.530G/S ONSET.

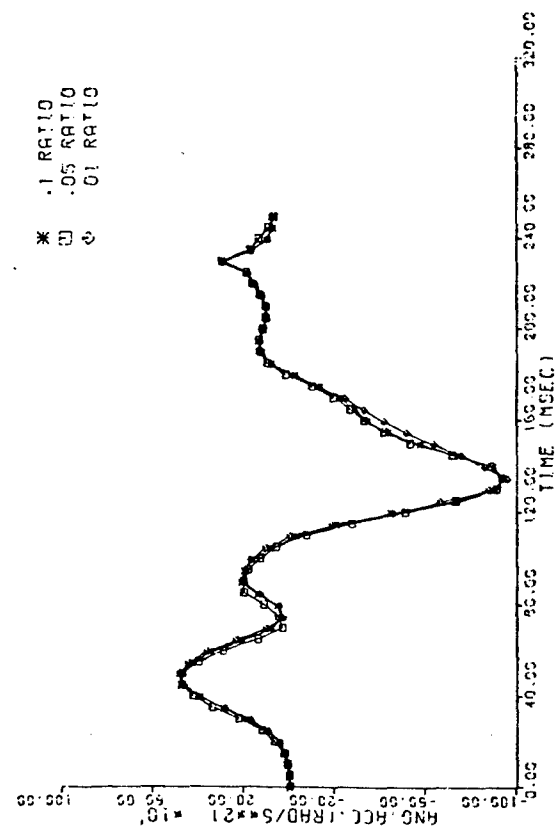


Fig. 6 - Ratio test comparison for head angular acceleration results (CVSLA)

SIM H182.9.80-PK.530G/S ONSET.

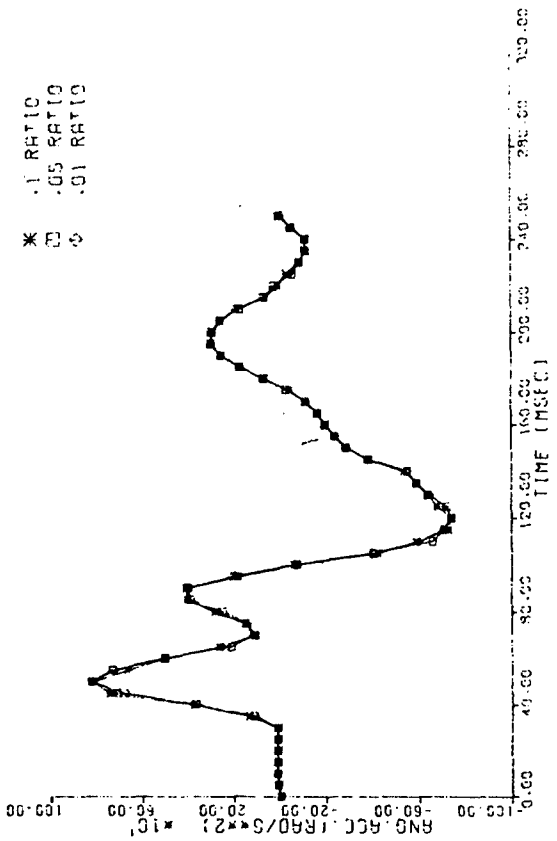


Fig. 7 - Ratio test comparison for head angular acceleration results (Prometheus)

SIM H182.9.80-PK.530G/S ONSET.

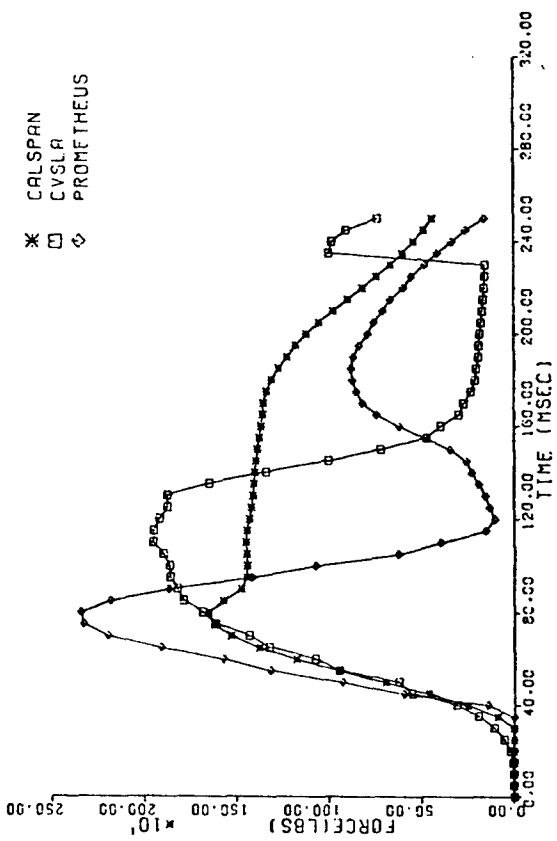


Fig. 8 - Lap belt loads

a ratio test of 0.05 and a 0.1 ms. minimum step size, no check on the 0.1 ratio test was conducted. Both CVSLA and Prometheus calculate error bounds for each variable, comparing them at each time step with the difference between the predicted and corrected values. Calspan on the other hand, has the option of using different ratio tests for the various variables. If no ratio test limit is provided for a given variable, no check is conducted on that variable and the convergence test for a given integration step can be passed despite possible inaccuracies or even instabilities in that quantity. All Calspan runs presented in this paper however, applied the ratio test quoted to the linear acceleration of the reference segment, as well as to the angular acceleration components of all 16 segments modeled. Intra-program outputs for the various ratio tests were compared for consistency and Figures 5, 6, and 7 show the results for the head angular acceleration, one of the most sensitive output variables. All Calspan and Prometheus outputs were virtually unchanged over the different ratio limits while CVSLA showed slight variation for the 0.05 ratio test, but appeared stable. The minimum permissible step sizes for Calspan and Prometheus were never reached, indicating that the variables passed the ratio tests without having to resort to the smallest step size provided. The CVSLA output was not extensive enough to determine whether the minimum allowable time intervals were approached, but the appreciable increases in program execution times with the lower ratio tests did preclude the chronic use of the minimum step size. Additionally, the virtually identical outputs for the 0.1 and 0.01 ratio tests (using minimum step sizes of 0.1 and 0.01 ms. respectively) indicates that the minimum time interval for these two runs was adequate. Inter-program comparisons presented below used ratio test limits of 0.05, 0.1, and 0.1 for Calspan, CVSLA, and Prometheus, respectively. The CPU time necessary to execute the programs depended strongly on the integration parameters. With all three programs integrating to 250 ms. typical CPU execution times on a CDC 6600, for the ratio test limits shown, ranged from 296 to 754 sec. for Calspan, from 132 to 354 sec. for CVSLA, and from 36 to 49 sec. for Prometheus.

Comparison Criteria - With the exception of minor program modifications to CVSLA to make inputs comparable, no rewriting of source code was conducted in any of the programs to change the respective mechanical idealizations. The programs, as delivered, were thoroughly checked out; sample problems were run, and the results compared to those obtained on other computer systems. Since results proved to be consistent, the programs were assumed to be error free and the differences in program results were attributed to the respective mechanical idealizations employed. Although convergence for the variables was checked, possible program errors, resulting in inaccuracies of the numerical solutions, cannot be absolutely ruled out as contributors to the differences in results. To elimi-

nate all possibility of program errors, all three simulators would have to be run and compared under identical conditions and mechanical idealizations (same number of segments, identical loading and unloading functions, etc.). The only major differences then would be the various integration procedures employed. A direct comparison of results under these conditions would isolate possible programming deficiencies as well as make a comparison of execution times more meaningful, since identical idealizations and comparable accuracy would have been used. Due to the user oriented nature of this paper, this analytic approach was not taken.

RESULTS

In order to make a direct comparison of the three programs possible, the head pivot and clavicular joints in the Calspan model were locked. Since Prometheus does not allow for a footrest, the modeled environment consisted solely of seat back, seat pan and floor surfaces. Consequently, with the exception of a somewhat different distribution of masses, the three representations of the test subject and interacting surfaces were as uniform as the various programs would allow. Differences in results should be due primarily to the methodologies used in modeling occupant-restraint interactions and joint loading and unloading characteristics. The results proved to be relatively consistent, although significant differences were evident, especially in the predicted belt loads. For the lap belt load (Figure 8) both CVSLA and Prometheus displayed higher amplitudes than Calspan, although the loading characteristics were quite similar. Calspan and Prometheus reached their peak forces at approximately the same time (80 ms.), whereas the corresponding CVSLA value was delayed by 35 ms. This delay was probably due to motion of the occupant under his restraint, since both Calspan and Prometheus assumed the lap belt to be anchored to the lower torso, while CVSLA allowed for submarining. Unloading characteristics of the lap belt were similar for CVSLA and Prometheus whereas Calspan had a much more gradual decrease in forces generated.

Shoulder strap loads (Figure 9) also demonstrated differences in occupant restraint interactions. CVSLA and Prometheus had similar frequencies of oscillation with the latter damping out much more rapidly. This damping is also evident in Calspan, although the frequency was higher than in the other two, indicating a stiffer interface. It must be remembered that these variations are primarily due to the different force deflection models employed by the respective programs. Although all three programs use tabular input in defining loading characteristics, they differ in their treatment of the unloading algorithm. Prometheus employs a fixed tabular input and CVSLA a fixed polynomial approximation. Calspan on the other hand uses a dynamic unloading process based on energy absorption and energy restitution coef-

SIM H182.9.8C-PK.530G/S ONSET.

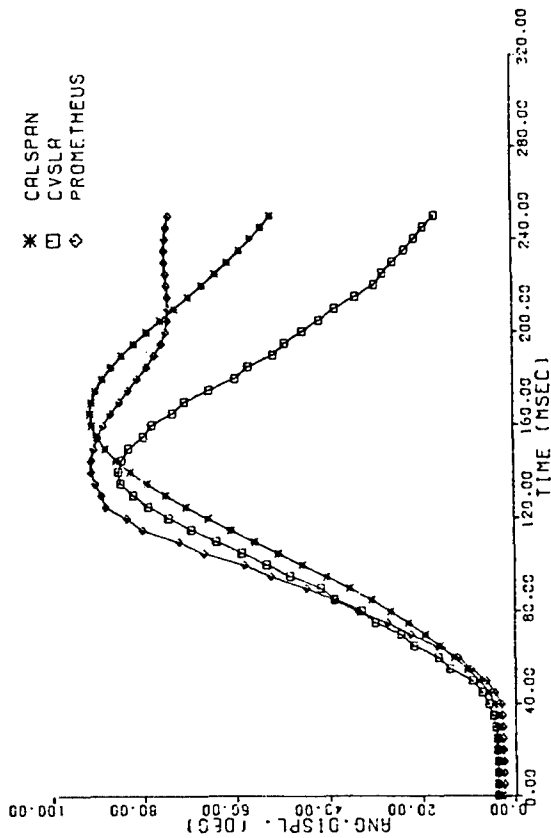


Fig. 11 - Neck angular displacement

SIM H182.9.8C-PK.530G/S ONSET.

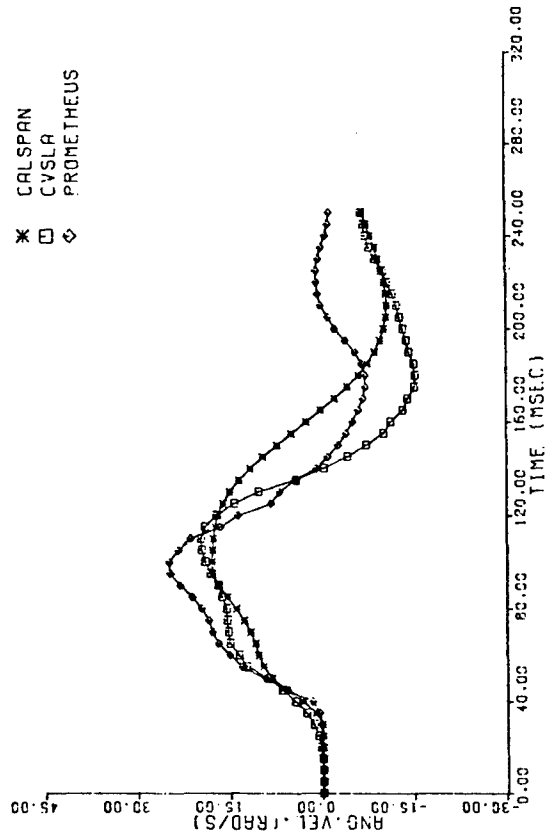


Fig. 12 - Head angular velocity

SIM H182.9.8C-PK.530G/S ONSET.

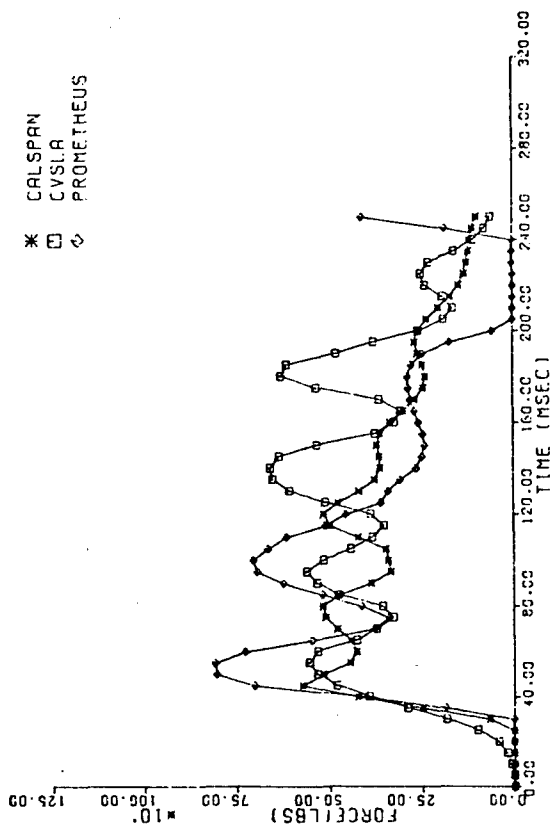


Fig. 9 - Shoulder strap loads

SIM H182.9.8C-PK.530G/S ONSET

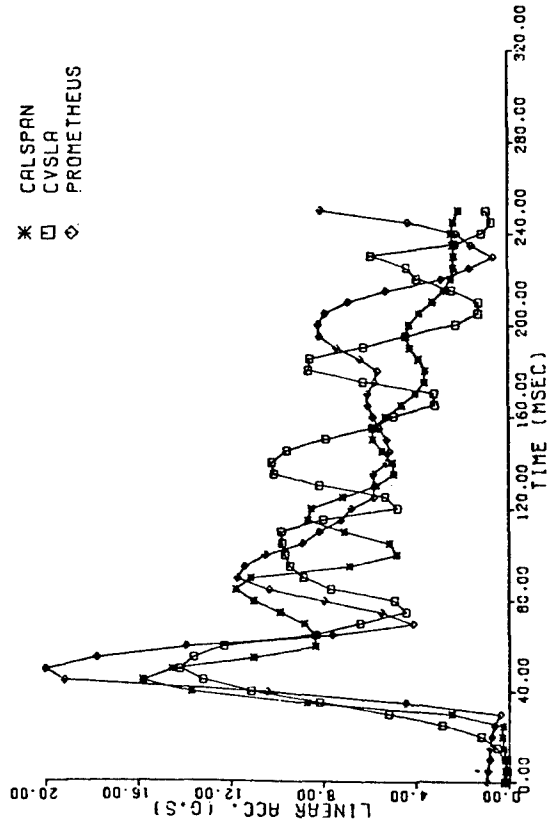


Fig. 10 - T1 resultant linear acceleration

ficients. It appears that the bulk of the variation in results can be attributed to the different treatments of hysteresis.

This variation in loading of the shoulder straps was reflected in the T1 accelerations (Figure 10). CVSLA and Calspan agreed well in initial accelerations achieved, and time of peak loading, but different frequencies of oscillation were again evident, with the latter being more damped. Prometheus proved to be similar to Calspan but indicated a greater initial G level than was predicted by the other two.

Since the head-neck system was rigid in all cases, the neck angular displacement can be considered coincident with head angular displacement. Neck angular displacement results (in the inertial reference frame) are shown in Figure 11. Since neck-thorax joint ranges were identical, variability in neck angular displacements attained were a result of differences in the respective forcing functions (T1 acceleration) as well as variability in the joint loading calculations once the limits had been reached. Calspan and Prometheus results displayed a larger excursion than CVSLA, indicating a softer joint stop.

Head angular velocity and acceleration (Figures 12 and 13) were similar in both the magnitudes attained as well as in their time histories. Calspan and CVSLA head angular velocities were comparable in the initial stages with differences in the later values probably due to unloading of the joint stops. Prometheus although attaining a larger initial value, generally replicated the results. Trends in head angular accelerations were also consistent in all the simulations. All exhibited the characteristic initial bi-phasic time history followed by a reversal in head-neck rotation as the neck joint unloaded. Oscillations in linear acceleration evident at T1 were relatively damped out upon reaching the head C.G. (Figure 14). Prometheus again tended to give the highest predicted G level attained but the trends exhibited by all three programs were similar.

Although results described do indicate good correlation in trends and magnitudes, the relevant question as to the validity of these simulations still had to be addressed. Predicted neck angular displacements were compared to the human data (NAMRL) and of the three programs Calspan results (LOCK-HP,CL) were found to give the closest approximation (Figure 15). It is crucial to remember that neck angle was defined as the angle a vector extending from T1 origin to the occipital condylar point makes with the inertial reference frame. What this result indicates is that the simulation was quite accurate in predicting the relative displacement between T1 and the occipital condylar point. Consequently, if the head-neck system were in fact rigid, the simulation (as far as predicting head and neck motion) could be considered a success in that the head angular displacement would by definition be just as accu-

rate. Human head to neck angular displacement (that is, the angle the neck vector makes with the head anatomical coordinate system) is shown in Figure 16. This analysis showed that by the definition of head and neck used in this paper there did exist head-neck dorsiflexion, reaching a value of approximately 37 degrees (NAMRL). Consequently, since relative head-neck motion is evident, articulation between the head and neck segments must be provided. Since only Calspan had this facility, both the clavicles and the head pivot were sequentially unlocked and the program was rerun for these additional degrees of freedom (LOCK-HP and UNLOCKED respectively). The neck angular displacement results (Figure 15) were not significantly changed from the locked case. The absolute head angular displacement (Figure 17) preceded and exceeded that of the test case and since the neck angles agreed well, this error lies in the relative head to neck motion. The simulation head-neck angle did not achieve the degree of dorsiflexion that was indicated in the test data and demonstrated appreciable head-neck ventriflexion once the neck torso joint stop began loading (Figure 16).

It should be noted that only minimal head to neck dorsiflexion was attained by unlocking of the head pivot. In fact, for the first 140 ms. the absence of significant head-neck motion would indicate that UNLOCKED results should be in good agreement with the two locked joint simulations. Head angular velocity and acceleration did not differ significantly for the locked vs. unlocked cases (Figures 18 and 19), although unlocking of the head pivot and clavicles did delay the corresponding curve. In relation to the test data, the head angular velocity of the unlocked joints case was of lower magnitude with slower rise and decay times while the head angular accelerations failed to replicate the high initial amplitude and following overshoot. Results of the head resultant linear acceleration were generally poor in that although the bi-phasic aspect of the test curve was evident, the magnitudes differed significantly (Figure 20). T1 linear acceleration proved reasonable for the first half of the simulation, exhibiting similar trends and amplitudes achieved (Figure 21).

SUMMARY AND CONCLUSIONS

Although simulation results from the various programs agreed well, their accuracy in replicating the test data was generally poor. Inter-program correlations could be improved by further adjustments to the input parameters but the basic problem of inconsistency with test results would still remain unresolved. Possible improvements to increase sensitivity include greater sophistication in modeling occupant-environment (seating and restraint system) interactions. Submarining and contacts with cabin surfaces affect

SIM H182.9.80-PK.530G/S ONSET.

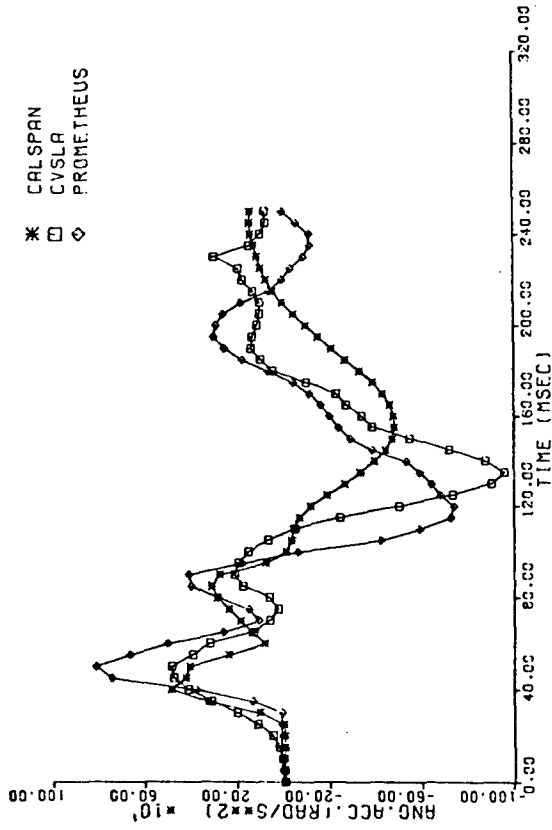


Fig. 13 - Head angular acceleration

SIM H182.9.80-PK.530G/S ONSET.

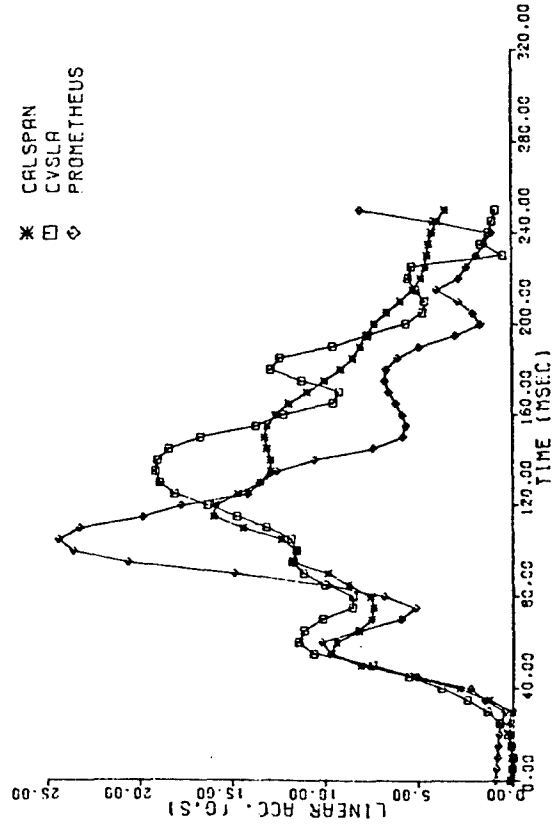


Fig. 14 - Head resultant linear acceleration

SIM H182.9.80-PK.530G/S ONSET.

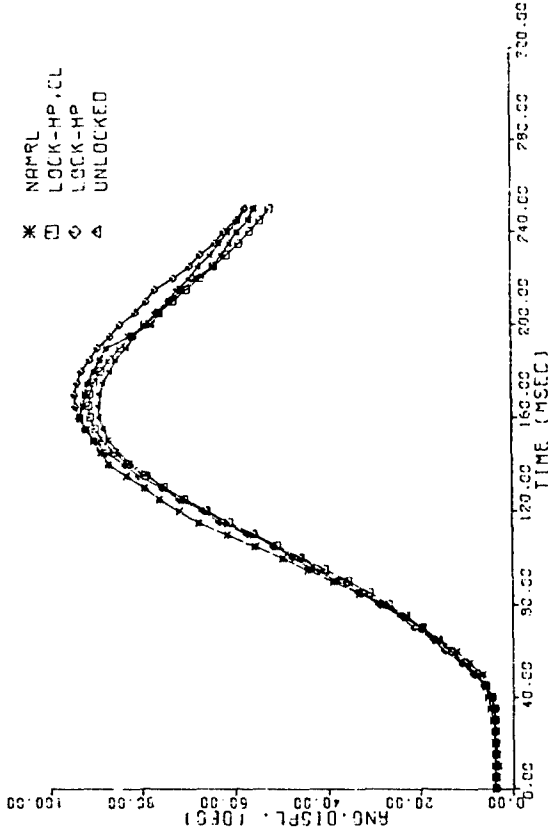


Fig. 15 - Neck angular displacement

SIM H182.9.80-PK.530G/S ONSET.

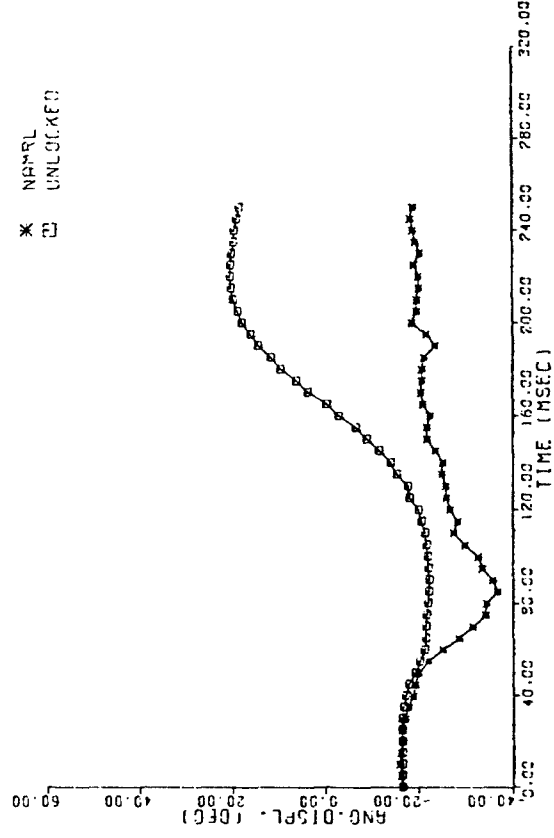


Fig. 16 - Head-neck angular displacement

SIM H182.9.8G-PK.530G/S ONSET.

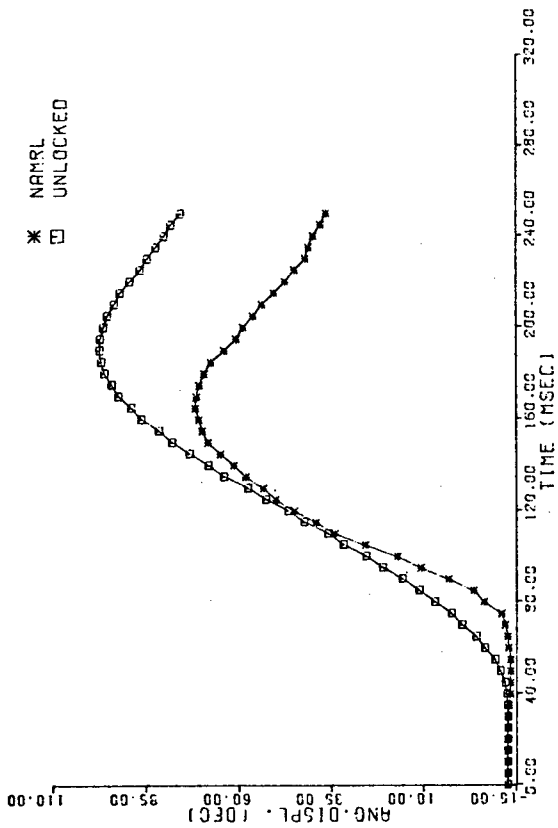


Fig. 17 - Head angular displacement

SIM H182.9.8G-PK.530G/S ONSET.

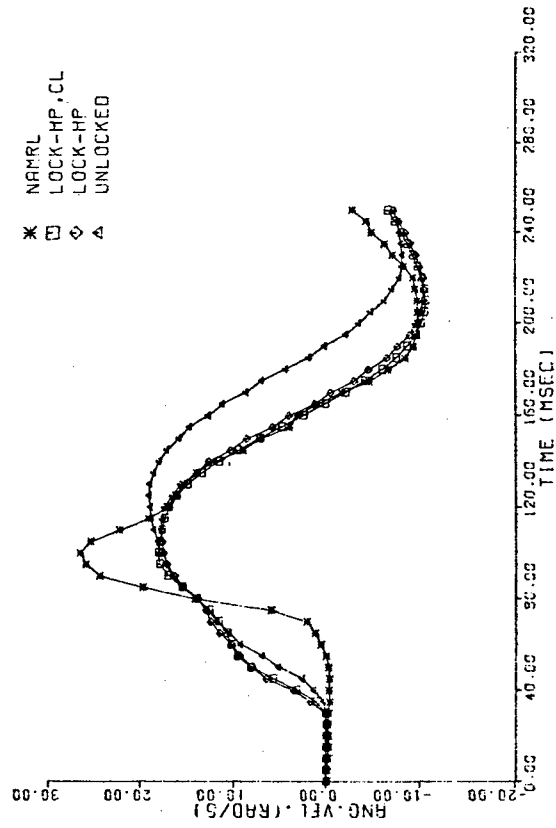


Fig. 18 - Head angular velocities

SIM H182.9.8G-PK.530G/S ONSET.

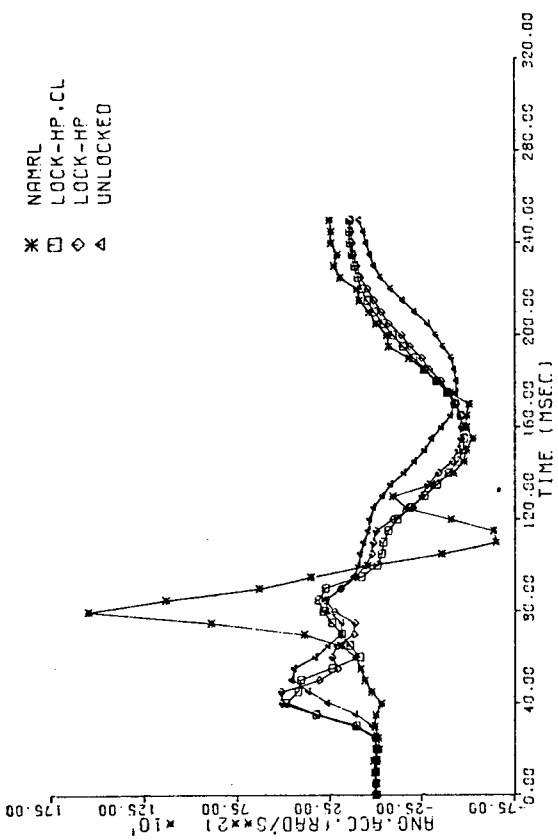


Fig. 19 - Head angular accelerations

SIM H182.9.8G-PK.530G/S ONSET.

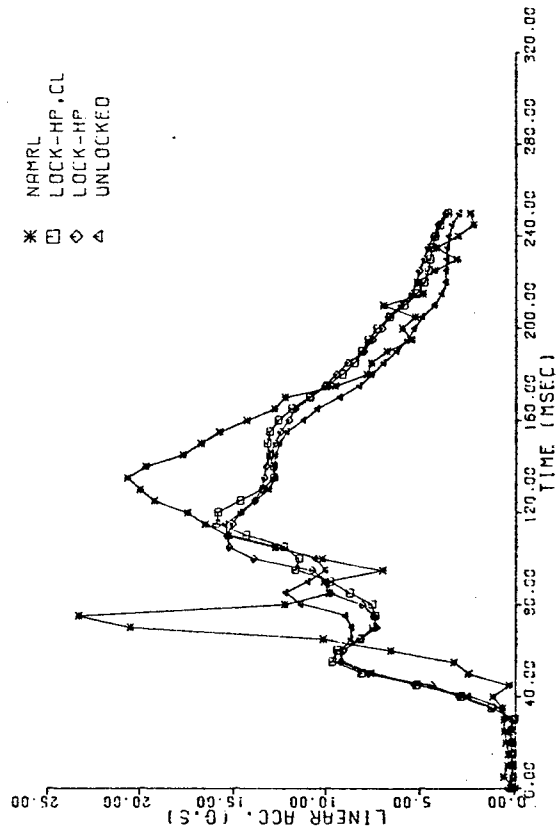


Fig. 20 - Head resultant linear accelerations

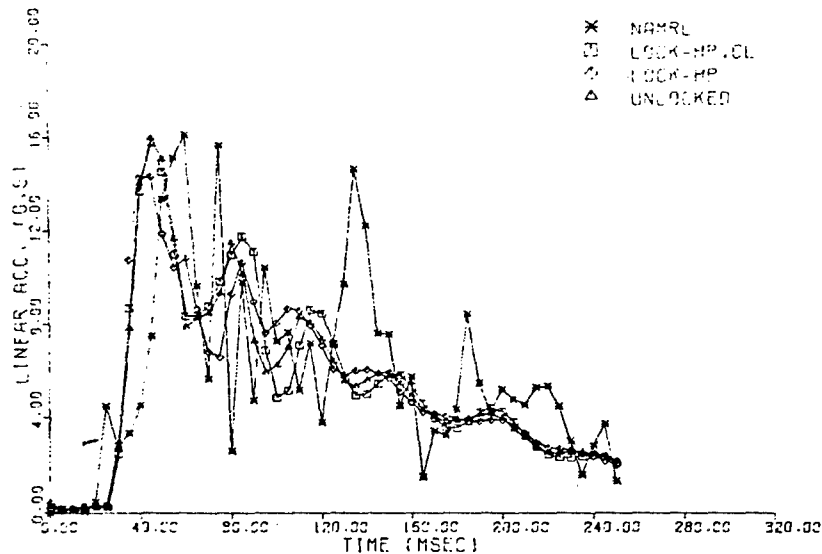


Fig. 21 - T1 resultant linear accelerations

results and should consequently be included in models that hope to address general applications. Although user oriented features have some very obvious advantages, the loss of the ability to model specifics can decrement usage as well as degrade the results obtained. The intended usage of the programs will affect the degree of sophistication required. If structural response is of prime interest, then occupant simulation need not approach the complexity that would otherwise be warranted. If that is the case however, conclusions about the response of that occupant to decelerative pulses should be made with great caution.

Lack of precise input parameters still represents one of the most vexing problems. Relatively small errors in joint ranges and loading and unloading properties as well as force deformation characteristics of the various interacting surfaces can significantly change results. Since great care was taken in making inputs to the three programs comparable, results were generally consistent if not accurate. Additional sophistication is warranted since the resulting simulation results did not approximate those of the test. The inclusion of additional articulation between the head and neck did not resolve the problem in that greater accuracy was not achieved. This is not to say that simulation of relative motion between the head and neck segments is unnecessary. Human head-neck values clearly indicated that relative motion between the head and neck does in fact take place. Since increased articulation, by itself, did not provide the expected displacements, other modifications have to be considered. It must be remembered that neck angular displacements agreed very well and consequently discrepancies in the head angular displacement must be accounted for relative to the occipital condyles. Although the occipital

condyles are generally considered the anatomical pivot point, it need not necessarily be the mathematical one. Since the head does not rotate on the neck at a well defined point but slides and rolls on the atlas, the center of rotation of this complex motion would define the precise pivot. If this theoretical pivot lies somewhere above the head C.G., then the demonstrated head-neck dorsiflexion could be achieved due to the revised geometry. Additionally, the representation of the neck as a rigid segment is an oversimplification that would affect head results. The introduction of a flexible neck would probably elevate (due to whiplash) the acceleration levels achieved but should not in itself reverse direction of motion.

The time history of the human data showed that peak T1 linear acceleration was followed by peak angular and linear accelerations of the head, indicating that forces to the head are propagated through T1. It is interesting to note that maximum head-neck dorsiflexion is attained at approximately 85 ms., and that peak head linear and angular acceleration occur at 75 and 79 ms., respectively. Since the peak accelerations and maximum head-neck angular displacement (dorsiflexion) are almost coincident in time, these peak accelerations appear to be caused by head-neck pivot loading. This theorized loading-unloading of the head-neck joint is consistent with head angular acceleration data where unloading produces the overshoot exhibited at approximately 110 ms. Additionally, a sharp spike is also evident in the T1 linear acceleration profile at approximately 80 ms., further substantiating possible head-neck loading. Since variability between simulation (UNLOCKED) and human test results became evident approximately 40-60 ms. into the pulse, muscular contraction (whose response time would be in this domain) could

account for the dorsiflexion of the head relative to the neck. Alterations to the program to substantiate this hypothesis, together with inclusion of a flexible neck, will be undertaken before sensitivity analysis and parameter adjustments will be conducted.

ACKNOWLEDGEMENTS

The authors wish to express their gratitude to Dr. J. Fleck (Calspan Corp.), Dr. D. Laananen (Mech. Engr. Dept., The Pennsylvania State University), Mr. I. Kaleps (Biodynamics and Bionics Div., Wright-Patterson AFB), Mr. R. Karnes (Boeing Computer Services, Inc.), and Dr. L. Ovenshire (Office of Vehicle Safety Research, NHTSA), without whose help and advice this paper would not have been possible.

REFERENCES

1. C.L. Ewing, D.J. Thomas, G.W. Beeler, L.M. Patrick, and D. B. Gillis, "Dynamic Response of the Head and Neck of the Living Human to -Gx Impact Acceleration." Paper No. 680792, Proceedings of Twelfth Stapp Car Crash Conference. New York: Society of Automotive Engineers, Inc., 1968
2. C.L. Ewing, D.J. Thomas, "Human Head and Neck Response to Impact Acceleration." Naval Aerospace Medical Research Laboratory Detachment, New Orleans, Monograph 21, Aug. 1972.
3. L.B. Walker, E.H. Harris, U.R. Pontius, "Mass, Volume, Center of Mass, and Mass Moment of Inertia of Head and Neck of Human Body." Paper No. 730985, Proceedings of Seventeenth Stapp Car Crash Conference. New York: Society of Automotive Engineers, Inc., 1973.
4. W.T. Dempster, "Space Requirements of the Seated Operator." Report 55-159, Wright Air Development Center, Air Research and Development Command, Wright-Patterson AFB, 1955.
5. A.D. Glanville, G. Kreezer, "The Maximum Amplitude and Velocity of Joint Movement in Normal Male Human Adults." Hum. Biol., Vol. 9 (1937), pp. 197-211.
6. B.M. Bowman, D.H. Robbins, "Parameter Study of Biomechanical Quantities in Analytical Neck Models." Paper No. 720957, Proceedings of Sixteenth Stapp Car Crash Conference, New York: Society of Automotive Engineers, Inc., 1972.
7. C. Tarriere, C. Sapin, "Biokinetic Study of the Head to Thorax Linkage." Paper No. 690815, SAE Transactions, Vol. 78, 1969.
8. E.B. Becker, "Preliminary Discussion of an Approach to Modeling Living Human Head and Neck to -Gx Impact Acceleration." Human Impact Response, pp. 321-328, Plenum Publishing Corp., 1973.
9. C.K. Kroell, D.C. Schneider, A.M. Nahum, "Impact Tolerance and Response of the Human Thorax II." Paper No. 741187, Proceedings of Eighteenth Stapp Car Crash Conference, New York: Society of Automotive Engineers, Inc., 1974.
10. G. Kourouklis, J.J. Glancy, S.P. Desjardins, "The Design, Development, and Testing of an Aircrew Restraint System for Army Aircraft." USAAMRDL Tech. Report 72-26, Fort Eustis, VA, 1972.
11. J.A. Bartz, F.E. Butler, "A Three Dimensional Computer Simulation of a Motor Vehicle Crash Victim." Report No. VJ-2978-V-2, Volume 1 - Volume 4, Calspan Corp., Transportation Research Dept., Buffalo, New York, 1972.
12. J.T. Fleck, F.E. Butler, and S.L. Volgel, "An Improved Three Dimensional Computer Simulation of Crash Victims." Volume 1 - Volume 4. Final Report for Contract No. DOT-HS-053-2-485, DOT Report Nos. DOT-HS-801 507 through 510, NHTSA, April 1975.
13. J.T. Fleck and F.E. Butler, Monthly Progress Report for February 1976. Submitted to NHTSA by the Calspan Corporation for Contract No. DOT-HS-6-01300. Validation of Crash Victim Simulator (unpublished).
14. D.H. Laananen, "Development of a Scientific Basis for Analysis of Aircraft Seating Systems." Report No. 1510-74-36, Ultrasystems, Inc., Dynamic Science Division, Phoenix, AZ, 1974.
15. D.W. Twigg, R.N. Karnes, "Prometheus - A User Oriented Program for Human Crash Dynamics." Report No. BCS40038, Boeing Computer Services, Inc., Space and Military Applications Division, Seattle, Washington, 1974.
16. R.N. Karnes, J.L. Tocher, and D.W. Twigg, "Prometheus - A Crash Victim Simulator." Aircraft Crashworthiness, University Press of Virginia, pp. 327-346, 1975.